FRAGILITY FUNCTIONS OF DIFFERENT BRIDGE TYPES SUBJECT TO SEISMIC SHAKING AND LATERAL SPREADING

J. Zhang[1], Y. Huo[2], S.J. Brandenberg[3] and P. Kashighandi[4]

[1,3] *Assistant Professor,* [2,4] *Graduate Student Researcher, Dept. of Civil and Environmental Engineering , University of California, Los Angeles, USA*
Email: zhangj@ucla.edu, huoyili@ucla.edu, sjbrandenberg@ucla.edu, pirooz@ucla.edu

ABSTRACT :

Bridges, as the most critical component in transportation system, have suffered various levels of damages due to strong shaking or liquefaction-induced spreading in past earthquakes. This paper evaluates seismic vulnerability of six classes of typical bridges in California, whose failure mechanisms and damage resistant capability are different due to varying structural configurations, namely superstructure type, connection, continuity at support and foundation type etc. Nonlinear time history analyses are conducted on bridge models subjected to a suite of 250 recorded earthquake motions with increasing intensity. A static pushover procedure is also implemented to evaluate the vulnerability of the bridges when subjected to liquefaction-induced lateral spreading. Fragility functions for each class of bridges are derived and compared for both seismic shaking (based on time history analyses) and lateral spreading (based on equivalent static procedure) for different performance states. The study finds that the fragility functions due to either ground shaking or lateral spreading show significant correlation with the structural characterizations, but differences emerge for ground shaking and lateral spreading conditions.

KEYWORDS: Bridge, seismic, liquefaction, lateral spreading, fragility function

1. INTRODUCTION

Highway bridges have shown to be susceptible to damages during past major earthquakes. Increased horizontal and vertical load due to dynamic effects under seismic shaking is attributed as the most dominant cause for the observed bridge damages (Basöz and Kiremidjian 1998). The pier column failure of Hanshin expressway during the 1995 Kobe earthquake (Priestley et al, 1996) and collapse of Cypress Street Viaduct during 1989 Loma Prieta earthquake (Chen and Duan, 2003) are examples of failures due to excessive seismic loading. For bridges built on liquefiable soil, earthquake induced liquefaction and lateral spreading have attributed to foundation weakening/failure and subsequent superstructure damages. The span unseating of Nishinomiya Bridge during 1995 Kobe earthquake (Wilson, 2003) and collapse of Showa Bridge during 1964 Niigata earthquake (Yasuda and Berrill, 2000) are examples of spectacular failures caused by liquefaction. Nevertheless, there are many bridges that have performed reasonably well under either seismic shaking or lateral spreading. For example, the Landing Road Bridge suffered only moderate and reparable damage despite as much as 2.0 meters of lateral spreading of the surrounding soils during the 1987 Edgecumbe earthquake (Berrill et al, 2001). It is observed that the detailed structural configurations (e.g. column detailing, superstructure type, material, connection, continuity at support and foundation type etc.) render different damage resistant capability for bridges. Furthermore, the failure mechanisms of bridges exhibited by seismic shaking or liquefaction-induced lateral spreading inevitably show different patterns due to distinctive load transferring mechanisms, resulting in difference of damage potential under these two situations. Therefore, it is important to evaluate the damage potential of different classes of bridges under seismic shaking and liquefaction-induced lateral spreading so that sound judgment can be made in terms of choosing appropriate design or retrofit measures to improve bridge response during earthquakes.

There are inherent variability and uncertainties associated with the seismic response of bridges due to either shaking (e.g. structural properties, earthquake motions etc.) or liquefaction-induced lateral spreading (soil properties, liquefaction mechanism and ground movement etc.). Under a probabilistic framework, this paper adopts the fragility function method to provide a comprehensive evaluation of bridge performance under seismic shaking or lateral spreading. The fragility functions of six classes of bridges are generated and compared to evaluate the effects of structural characterizations on damage probability of bridges. Nonlinear dynamic time history analyses are used to derive the fragility functions of bridges under seismic shaking while a static procedure is used to derive the fragility functions of bridges under liquefaction-induced lateral spreading. The important structural and foundation parameters are also identified.

2. BRIDGE RESPONSE UNDER SEISMIC SHAKING

2.1. Bridge Types and Numerical Modeling

The typical bridge designs were evaluated by reviewing drawings of numerous bridges obtained from Caltrans and six bridge models, as shown in Figure 1a-f, are selected to represent the common highway bridge types. Model E1 represents a continuous bridge with monolithic abutments. Contrast to model E1, model E2-E6 are all with seat-type abutments. Model E2 represents a continuous bridge with seat-type abutments. Model E3 is similar to Model E2 except with an expansion joint at the center of mid-span. Model E4 is isolated at the pier tops with continuous deck while model E5 has an expansion joint at mid-span in addition to the isolation. In model E6, simply supported connections are adopted at pier top and the adjacent decks are pin connected to prevent collapse. The structural properties of bridge components are taken from two real Caltrans bridges that were built before 1971. Previous study (Zhang et al. 2008) has shown that the location of expansion joints has no obvious effect on bridge response, so in this study their location are not varied.

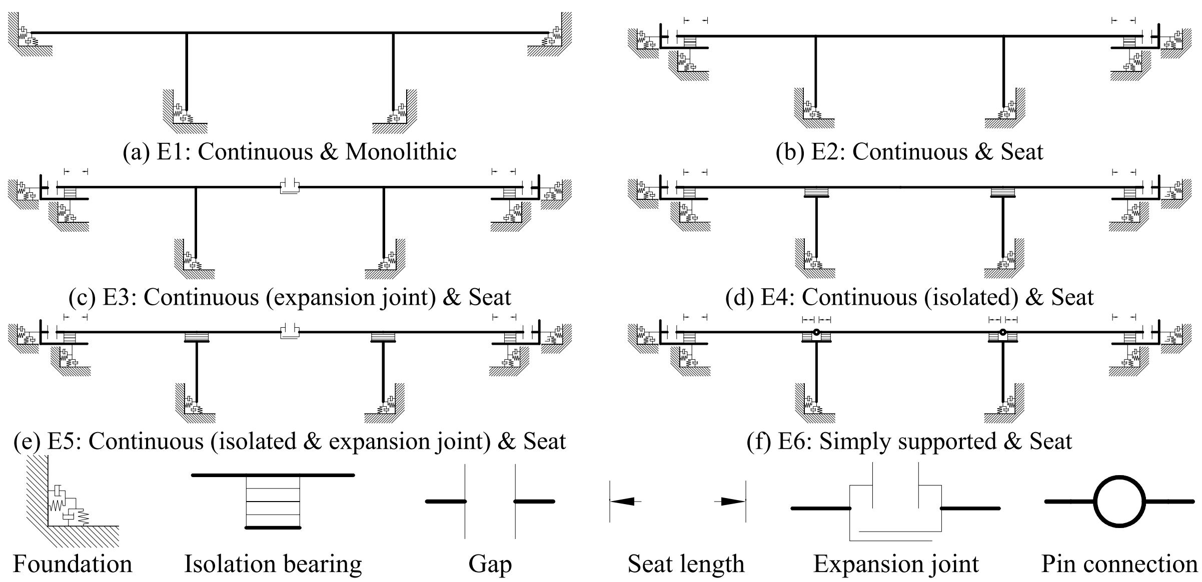

(g) Component legend

Figure 1 Sketch of six types of bridges

Numerical models are generated in software platform OpenSees (Mazzoni et al. 2006). Elastic beam elements are used for bridge deck and nonlinear fiber section beam elements are used to model the pier columns. The RC column has 72 in diameter and is reinforced with 26#11 longitudinal bars and #4 transverse reinforcements at 12 in interval. The column has a elastic stiffness of 1.10×10^5 *kN/m* and characteristic strength of 1.36×10^3 *kN*. This represents a typical design for bridges built before 1971. The middle span is 30m long while the other two spans are 20m each. Seismic isolation bearings are modeled with bilinear springs for horizontal load-carrying properties and elastic springs for vertical properties (Kumar and Paul 2007). The bearing parameters are selected based on the optimum design parameters as presented in Zhang and Huo (2008). Gap elements are employed to simulate the gap closing and the effects of pounding between deck and abutment. The seat length during earthquake shaking and lateral spreading is monitored and the analysis will be terminated if the seat length is reduced to zero. The soil structure interaction (SSI) is simulated with springs and dashpots representing the stiffness and damping of foundations supporting pier columns and embankment at end abutments, whose properties are determined by the methods presented by Zhang and Makris (2002a,b).

2.2. Fragility Functions of Bridges Under Seismic Shaking

The dynamic fragility functions of bridges can be numerically obtained through nonlinear time history analyses that account for the uncertainties in both seismic input motions and structural properties. Two computational methods, namely the probabilistic seismic demand analysis (PSDA) and the incremental dynamic analysis (IDA) are widely used to derive the fragility functions. PSDA relates the engineering demand parameter (EDP) to the intensity measure (IM) of earthquake record through an logarithm relationship and obtains the fragility function parameters by assuming the form of fragility curves (Mackie and Stojadinović, 2003, 2007). IDA derives the fragility functions by counting the damage cases for each IM level from the time history analyses of bridges using ground motions scaled to the same intensity level (Karim and Yamazaki, 2001).

In this paper, 250 sets of earthquake records are selected for both PSDA and IDA and the records are inputted in transverse, longitudinal and vertical direction simultaneously during analyses. Peak ground acceleration (PGA) is adopted as IM for earthquake input. The damage in pier columns and bearings are monitored and Table 2.1 lists the EDP, damage index (DI), damage state (DS) and corresponding limit state (LS) definitions for these two critical components.

Table 2.1 Probability of parameters of soil profile and foundation modeling

	EDP or DI definition	Slight damage (DS=1)	Moderate damage (DS=2)	Extensive damage (DS=3)	Collapse damage (DS=4)
Pier column (Choi et al, 2004)	Section ductility μ	$\mu>1$	$\mu>2$	$\mu>4$	$\mu>7$
Bearing	Shear strain γ	$\gamma>100\%$	$\gamma>150\%$	$\gamma>200\%$	$\gamma>400\%$

During earthquake, piers and bearings can experience different damage states, leading to a comprehensive damage state which is hard to describe by only one component DI. Previous studies suggest that a system fragility can be derived based on the functionality or repair cost after earthquake (Mackie and Stojadinović, 2007), or can be generated based on component level fragility (Nielson and DesRoches, 2007). In this study, a composite damage state (DS) is developed as shown in Eqn. 2.1. The proportion ratio 0.75 for columns and 0.25 for isolation devices are determined synthetically by considering the relative component importance for load-carrying capacity during earthquake and the repair cost after earthquake.

$$DS = \begin{cases} \operatorname{int}\left(0.75 \cdot DS_{Pier} + 0.25 \cdot DS_{Bearing}\right) & DS_{Pier}, DS_{Bearing} < 4 \\ 4 & DS_{Pier} \text{ or } DS_{Pier} = 4 \end{cases} \tag{2.1}$$

It is noted that the IDA method is generally more reliable than the PSDA method because the fragility functions are based on many more simulation cases and no pre-assumed relationship between the EDP and IM . Therefore this paper employs IDA to generate fragility curves. Nonlinear time history analyses are conducted for each bridge model subject to 250 sets of records scaled at 25 PGA levels ranging from 0.06g to 1.5g. The cumulative normal distribution function is applied to derive the fragility curve. Figure 2 compares the fragility curves of six bridge types shown in Fig. 1. The results show that models E2 and E3 perform least favorably among the six models and have much bigger damage probability than model E1 at same IM level. The more severe damage in models E2 and E3 can be attributed to the seat-type connection at abutments, which leads to smaller dynamic loads carried at abutments but more loads transferred to pier columns. In contrast to the seat-type abutment, the isolation at pier top reduces the damage experienced by pier columns, which is reflected by much lower fragility curves of model E4 and E5 than that of model E2 and E3. The expansion joint of model E3 does not make much difference in terms of the bridge response compared to model E2. Similar observation can be seen between models E4 and E5. Among all the models, it can be seen that model E1 performs best for earthquake intensity smaller than 0.7g while model E6 performs the best for earthquake intensity bigger than 0.7g for slight, moderate and extensive damage states. At collapse damage state, the model E1 is clearly the best structural type.

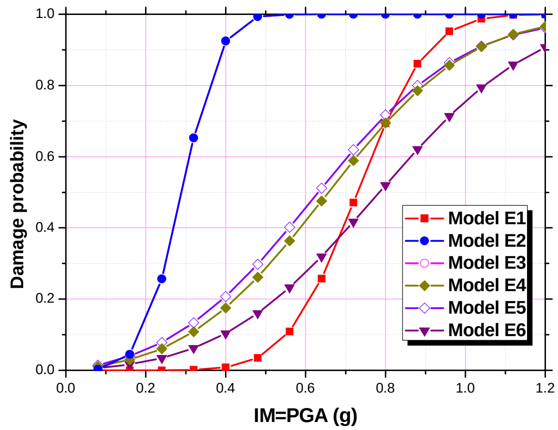

(a) Slight damage

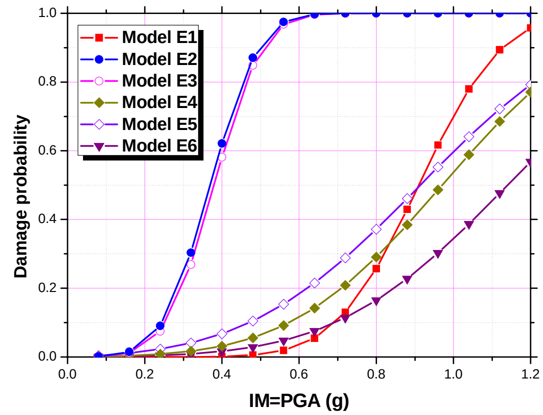

(b) Moderate damage

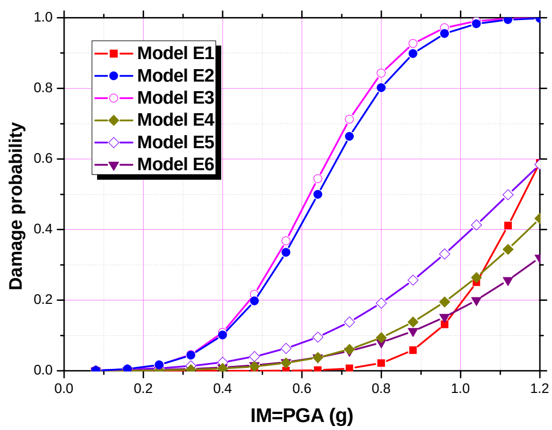

(c) Extensive damage

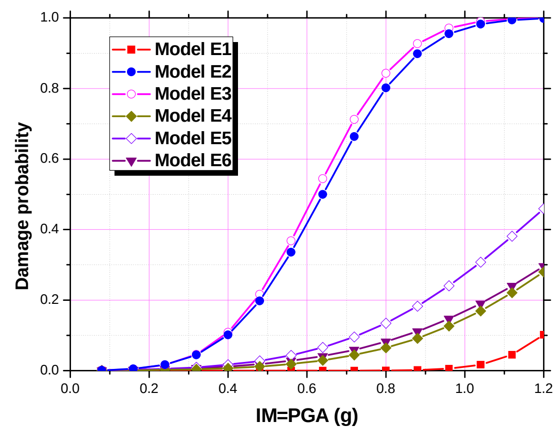

(d) Collapse damage

Figure 2 Fragility curves of six bridge models under seismic shaking

3. BRIDGE RESPONSE UNDER LIQUEFACTION-INDUCED LATERAL SPREADING

3.1. Procedure to Simulate Bridge Response Subject to Lateral Spreading

The above six bridge models are also evaluated for their performance under the liquefaction-induced lateral spreading. All superstructure details and properties are kept the same as in the previous section. The pile foundations are modeled by bilinear beam on Winkler foundation with p-y, t-z and q-z spring elements to simulate the soil lateral resistance, axial shaft friction and pile tip end bearing resistances respectively. The soil profile used in this study is representative of sites with a non-liquefiable clay crust over liquefiable loose sand and dense sand. Variations in the soil parameters were based on the USGS database of CPT soundings in the San Francisco bay area (USGS, 2007). Figure 3 presents the sketch of a bridge founded on the soil profile.

A static pushover analysis procedure proposed by Brandenberg et al (2007b) is employed to simulate the bridge response under liquefaction-induced lateral spreading. In this procedure, loading effect of the lateral spreading on bridge foundation is represented by imposing displacement demands from the spreading soils on the free ends of p-y springs attached to the bridge foundation. Inertia forces that are compatible with lateral spreading displacements using a Newmark sliding block method (Brandenberg et al, 2007a), are imposed on the superstructure and pile caps simultaneously with lateral spreading displacements.

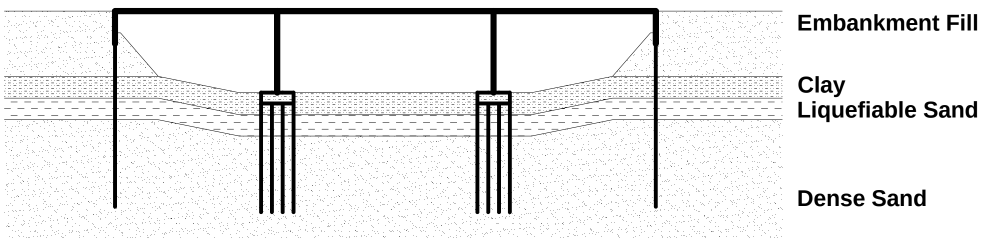

Figure 3 Sketch of simulation for bridge and soil profile with liquefiable sand layer

Figure 4 presents the deformed shapes of bridge model E1 under two possible load cases for liquefaction-induced lateral spreading. The results were obtained by imposing the displacements on the free ends of the p-y elements to model lateral spreading demands. In case I, lateral spreading happens in the left embankment, abutment foundation and left pier foundation. In case II, only the left pier foundation experiences lateral spreading displacement load. The analysis detail can be found in previous study (Brandenberg et al, 2008). For load case I, the pier damage is controlled by the second pier that was not exposed to lateral spreading due to a shift of the bridge superstructure from left to right. For load case II, the pier damage is controlled by the first pier where lateral spreading demand was imposed.

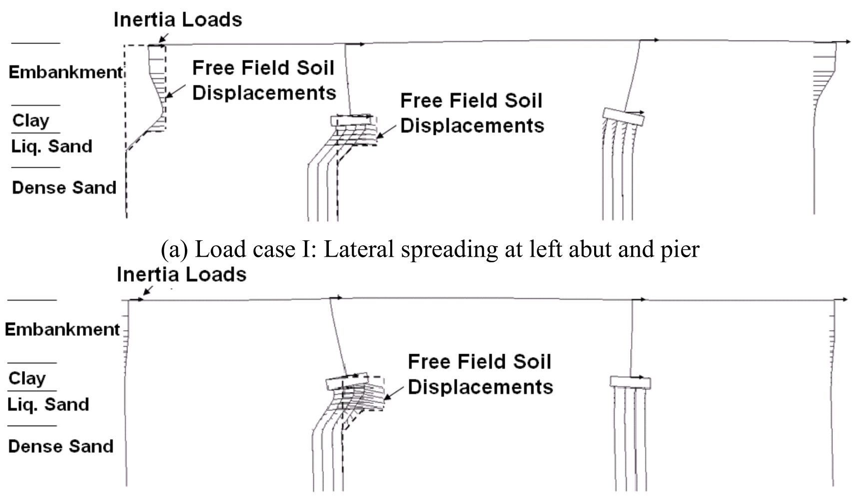

(a) Load case I: Lateral spreading at left abut and pier

(b) Load case II: Lateral spreading at left pier

Figure 4 Bridge deformation under two lateral spreading load cases

Due to insufficient information of soil profiles for various bridge locations, probabilistic properties of soil profiles are selected based on available data and the author's best judgment. Table 3.1 lists the probability properties of parameters used in soil profile and foundation modeling. As shown in the Table 3.1, 8 separated probabilistic parameters are considered in this study.

3.2. Fragility Functions of Bridges Under Liquefaction-Induced Lateral Spreading

Corresponding to static simulation procedure, First Order Second Moment (FOSM) and Monte Carlo methods are generally adopted to generate fragility functions. FOSM method assumes that both the input properties and output responses follow either normal or log-normal distributions, and applies only first order terms in Taylor's expansion to estimate the mean and standard deviation of response if the mean and standard deviation of the input properties are known (Christian, 2004). On the other hand, Monte Carlo method randomly selects a great number of input combinations of probability variables from the predetermined distribution, and uses these combinations to compute the distribution of the output response (Christian, 2004).

Table 3.1 Probability properties of parameters of soil profile and foundation modeling

Parameter		Median	Negative Variation	Positive Variation	Distribution
Crust thickness	Embankment	6.0m	4.5m	7.5m	Normal
	In situ clay	3.0m	1.5 m	4.5m	
Material strength		$\Phi'_{sand}=38^{o}$ $c'_{sand}=20$ kPa $c_{clay}=70$ kPa	Median×0.46	Median×2.17	Lognormal
$\Delta_{sand}/\Delta_{crust}$		0.5	0.16	0.84	Uniform
Liquefied sand m_p		0.050	0.025	0.075	Normal
y_{50} for p-y springs	Embankment	$y_{50}=0.20$ m	Median×0.5	Median×1.5	Normal
	In situ clay	$y_{50}=0.05$ m			
Axial capacity		Qtip=1020 kN	Median×0.5	Median×1.5	Normal
Inertia load		a=0.4g	a=0.2g	a=0.6g	Normal
Liquefied sand thickness		2.0m	1.0m	4.0m	Lognormal

Figure 5 depicts the fragility curves derived with Monte Carlo and FOSM method for bridge E1 under load case I. Two methods yield similar results. Therefore the FOSM method is adopted to save computational effort. The fragility curves of the six bridge models under lateral spreading are generated and compared in Figure 6. It is observed that the sequence of damage potential of the models under lateral spreading conditions is quite different with that under seismic shaking conditions. Among the six models, model E1 performs worst and model E5 performs best. Because the static load induced by lateral spreading at abutments and one pier is transferred to piers through the deck, the isolation bearings at both abutments and pier tops reduce the loads exerted on pier columns, and consequently mitigate the pier damage.

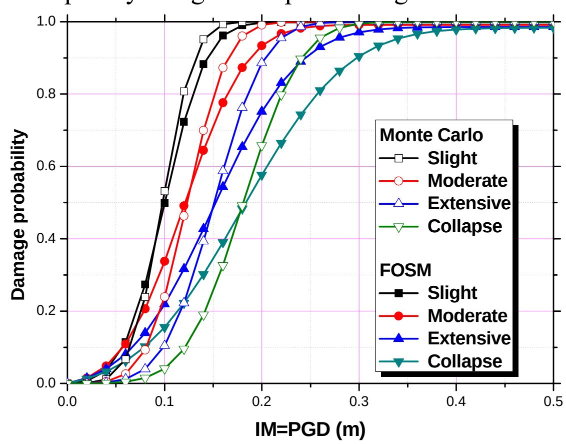

Figure 5 Fragility curves generated with Monte Carlo method or FOSM

4. CONCLUSIONS

In this study, the fragility functions of six different classes of bridges are derived when they are subject to seismic shaking or liquefaction-induced lateral spreading. The numerical models of bridges and their foundations were built in OpenSees environment to incorporate the soil-structure interaction effects and nonlinear behavior of columns, piles as well as connections. PSDA and IDA approaches are implemented to derive fragility curves under seismic shaking while FOSM and Monte Carlo methods are adopted to generate fragility curves under lateral spreading.

The study finds that the fragility functions of bridges subjected to either ground shakings or lateral spreading show significant correlation with the structural characterization. Under seismic shaking, the isolation at pier top benefits the bridge load-carrying capacities while seat-type abutment makes pier columns more vulnerable. Furthermore, simply support connections reduce the damage in pier columns. In contrast, under lateral spreading, the isolation at pier top and seat-type abutments protects pier columns from damage. It is possible that simply support connection leads more loads to pier columns than that of isolated continuous deck connection. The expansion joints do not significantly affect the damage probability under seismic shaking yet they improve the isolated bridge performance under lateral spreading. In summary, bridges have different resistant capacities to seismic shaking and lateral spreading and the difference can be explained with the different loading and load carrying mechanisms.

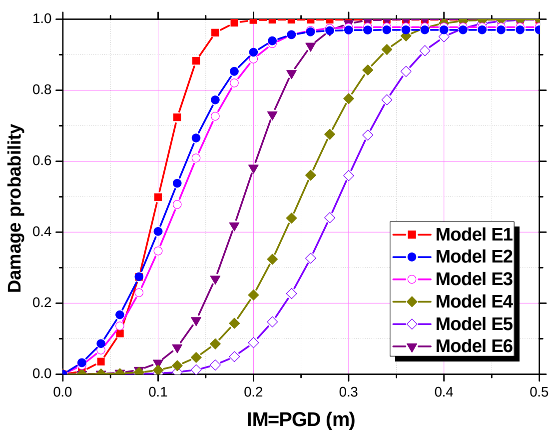

(a) Slight damage

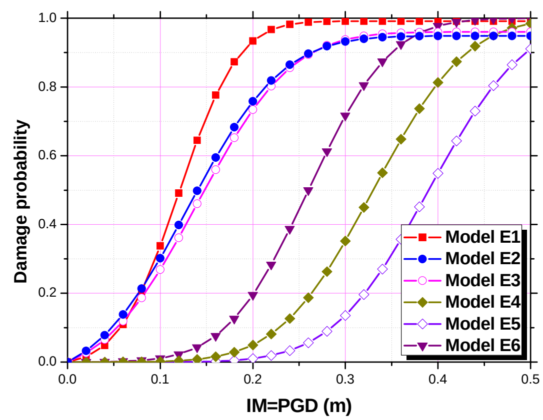

(b) Moderate damage

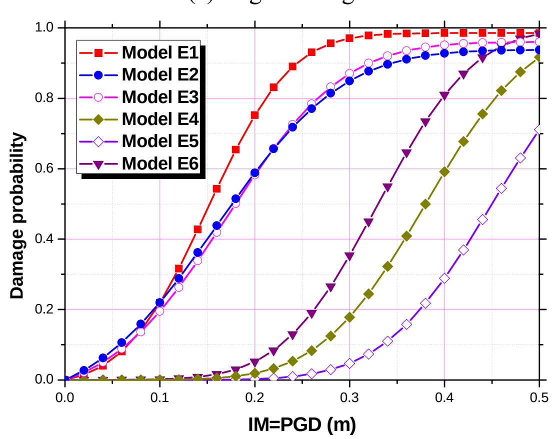

(c) Extensive damage

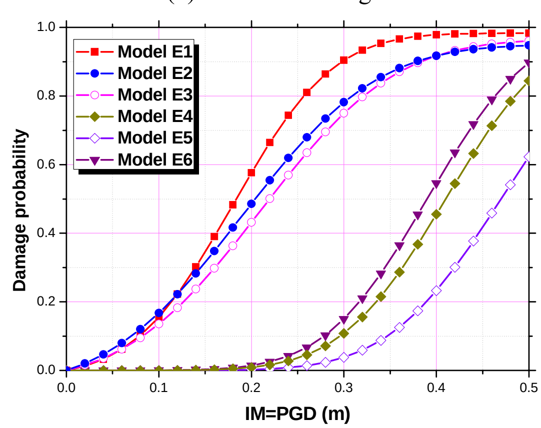

(d) Collapse damage

Figure 6 Fragility curves of six bridge models under lateral spreading

ACKNOWLEDGEMENT

Research funding for this work is provided by the Pacific Earthquake Engineering Research Center Lifelines program under project task No. 9C. Tom Shantz and Mark Yashinsky of Caltrans provided valuable help in developing the bridge classification system and providing as-built plans. The study utilized the computational resource at the San Diego Supercomputer Center (SDSC) through cyber-infrastructure resource allocation program.

REFERENCES

Basöz, N.I. and Kiremidjian, A.S. (1998). Evaluation of bridge damage data from the Loma Prieta and Northridge, CA earthquakes. *MCEER Report 98/04*. Multidisciplinary Center for Earthquake Engineering Research, University of California, Berkeley, USA.

Berrill, J.B., Christensen, S.A., Keenan, R.P., Okada, W., and Pettinga, J.R., (2001). Case study of lateral spreading forces on a piled foundation. *Geotechnique* **51:6**, 501-517.

Brandenberg, S.J., Boulanger, R.W., Kutter, B.L. and Chang, D. (2007a). Liquefaction induced softening of load transfer between pile groups and laterally spreading crusts. *Journal of Geotechnical and Geoenvironmental Engineering* **133:1**, 91-103.

Brandenberg, S.J., Boulanger, R.W., Kutter, B.L., and Chang, D. (2007b). Static pushover analyses of pile groups in liquefied and laterally spreading ground in centrifuge tests. *Journal of Geotechnical and Geoenvironmental Engineering* **133:9**, 1055-1066.

Brandenberg, S.J., Kashighandi, P., Zhang, J., Huo, Y. and Zhao, M. (2008). Sensitivity study of an older-vintage bridge subjected to lateral spreading. *Proceeding of 4th Geotechnical Earthquake Engineering and Soil Dynamics Conference*, Sacramento, USA, May, 2008.

Chen, W-F and Duan, L. (2003). Bridge Engineering: Seismic Design, CRC Press, New York, USA.

Christian, J.T. (2004). Geotechnical engineering reliability: how well do we know what we are doing? *Journal of Geotechnical and Geoenvironmental Engineering* **130:10**, 985-1003.

Choi, E., DesRoches, R. and Nielson, B. (2004). Seismic fragility of typical bridges in moderate seismic zones. *Engineering Structures* **26**, 187-199.

Karim, K.R. and Yamazaki, F. (2001). Effect of earthquake ground motions on fragility curves of highway bridge piers based on numerical simulation. *Earthquake Engineering and Structural Dynamics* **30**, 1839-1856.

Kumar, P.T.V. and Paul, D.K. (2007). Force-deformation behavior of isolation bearings. *Journal of Bridge Engineering* **12:4**, 527-529.

Mackie, K. and Stojadinović, B. (2003). Seismic demands for performance-based design of bridges. PEER *Report No.2003/16*. Pacific Earthquake Engineering Research Center, University of California, Berkeley, USA.

Mackie, K. and Stojadinović, B. (2007). Performance-based seismic bridge design for damage and loss limit states. *Earthquake Engineering and Structural Dynamics* **36:13**, 1953-1971.

Mazzoni, S., McKenna, F., Scott, M.H., Fenves, G.L., et al. (2006). OpenSees Command Language Manual. University of California, Berkeley, USA.

Nielson, B.G. and DesRoches, R. (2007). Seismic fragility methodology for highway bridges using a component level approach. *Earthquake Engineering and Structural Dynamics* **36**, 823-839.

Priestley, M.J.N., Seible, F. and Calvi, G.M. (1996). Seismic Design and Retrofit of Bridges, John Wiley & Sons, New York, USA.

United States Geological Survey (USGS). (2007). CPT data Alameda County. Online database: http://earthquake.usgs.gov/regional/nca/cpt/data/?map=alameda.

Wilson, J. C. (2003). Repair of new long-span bridges damaged by the 1995 Kobe earthquake. *Journal of Performance of Constructed Facilities* **17:4**, 196-205.

Yasuda, S., and Berrill, J.B. (2000). Observations of the earthquake response of foundations in soil profiles containing saturated sands. *Proceeding of GeoEng 2000 Conference*, Melbourne, Australia, November, 2000.

Zhang, J. and Huo, Y. (2008). Optimum isolation design for highway bridges using fragility function method. *Proceedings of 14th World Conference on Earthquake Engineering*, Beijing, China, October, 2008.

Zhang, J. and Huo, Y., Kashighandi, P. and Brandenberg, S.J. (2008). Effects of structural characterizations on fragility functions of bridges subjected to seismic shaking and lateral spreading. *Proceedings of the Sixth National Seismic Conference on Bridges and Highways*, Charleston, July, 2008.

Zhang, J. and Makris, N. (2002a). Kinematic response functions and dynamic stiffnesses of bridge embankments. *Earthquake Engineering and Structural Dynamics* **31**, 1933-1966.

Zhang, J., and Makris, N. (2002b). Seismic response analysis of highway overcrossings including soil-structure interaction. *Earthquake Engineering and Structural Dynamics* **31**, 1967-1991.